



ORIGINAL ARTICLE

OPEN

Sirtuin3 promotes the degradation of hepatic Z alpha-1 antitrypsin through lipophagy

Brittney Poole¹  | Regina Oshins¹ | Zhiguang Huo² | Alek Aranyos¹ | Jesse West¹ | Sergio Duarte³ | Virginia C. Clark⁴  | Thiago Beduschi³ | Ali Zarrinpar³ | Mark Brantly¹ | Nazli Khodayari¹

¹Department of Medicine, Division of Pulmonary, Critical Care and Sleep Medicine, University of Florida, Gainesville, Florida, USA

²Department of Biostatistics, College of Public Health, University of Florida, Gainesville, Florida, USA

³Department of Surgery, Division of Transplantation and Hepatobiliary Surgery, University of Florida, Gainesville, Florida, USA

⁴Department of Medicine, Division of Gastroenterology, Hepatology, and Nutrition, University of Florida, Gainesville, Florida, USA

Correspondence

Nazli Khodayari, Department of Medicine, Division of Pulmonary, Critical Care and Sleep Medicine, University of Florida, Gainesville, FL 32610, USA.
 Email: nazli.khodayari@medicine.ufl.edu

Abstract

Background: Alpha-1 antitrypsin deficiency (AATD) is a genetic disease caused by misfolding and accumulation of mutant alpha-1 antitrypsin (ZAAT) in the endoplasmic reticulum of hepatocytes. Hepatic ZAAT aggregates acquire a toxic gain-of-function that impacts the endoplasmic reticulum which is theorized to cause liver disease in individuals with AATD who present asymptomatic until late-stage cirrhosis. Currently, there is no treatment for AATD-mediated liver disease except liver transplantation. In our study of mitochondrial RNA, we identified that Sirtuin3 (SIRT3) plays a role in the hepatic phenotype of AATD.

Methods: Utilizing RNA and protein analysis in an in vitro AATD model, we investigated the role of SIRT3 in the pathophysiology of AATD-mediated liver disease while also characterizing our novel, transgenic AATD mouse model.

Results: We show lower expression of SIRT3 in ZAAT-expressing hepatocytes. In contrast, the overexpression of SIRT3 increases hepatic ZAAT degradation. ZAAT degradation mediated by SIRT3 appeared independent of proteasomal degradation and regular autophagy pathways. We observed that ZAAT-expressing hepatocytes have aberrant accumulation of lipid droplets, with ZAAT polymers localizing on the lipid droplet surface in a direct interaction with Perilipin2, which coats intracellular lipid droplets. SIRT3 overexpression also induced the degradation of lipid droplets in ZAAT-expressing hepatocytes. We observed that SIRT3 overexpression induces lipophagy by enhancing the interaction of Perilipin2 with HSC70. ZAAT polymers then degrade as a consequence of the mobilization of lipids through this process.

Abbreviations: AAT, alpha-1 antitrypsin; AATD, alpha-1 antitrypsin deficiency; CMA, chaperone-mediated autophagy; ER, endoplasmic reticulum; EV, extracellular vesicle; IF, immunofluorescence; IP, immunoprecipitation; MAM, mitochondria-associated membrane; mt-RNA, mitochondrial RNA; PLIN2, Perilipin2 (adipose differentiation-related protein); SIRT3, Sirtuin3; TEM, transmission electron microscopy; WT, wildtype.

Supplemental Digital Content is available for this article. Direct URL citations are provided in the HTML and PDF versions of this article on the journal's website, www.hepcommjournal.com.

This is an open access article distributed under the terms of the Creative Commons Attribution-Non Commercial-No Derivatives License 4.0 (CCBY-NC-ND), where it is permissible to download and share the work provided it is properly cited. The work cannot be changed in any way or used commercially without permission from the journal.

Copyright © 2024 The Author(s). Published by Wolters Kluwer Health, Inc. on behalf of the American Association for the Study of Liver Diseases.

Conclusions: In this context, SIRT3 activation may eliminate the hepatic toxic gain-of-function associated with the polymerization of ZAAT, providing a rationale for a potential novel therapeutic approach to the treatment of AATD-mediated liver disease.

INTRODUCTION

Alpha-1 antitrypsin deficiency (AATD) is a rare genetic disease resulting from a mutation in the *SERPINA1* gene that encodes the alpha-1 antitrypsin (AAT) protein.^[1] AAT, primarily produced by hepatocytes, is a key serine protease inhibitor in plasma.^[2] The “normal” allele for AAT is referred to as “M” and the most common pathogenic allele is referred to as “Z” (E342K), responsible for ~95% of disease manifestations.^[3,4] The Z mutation results in misfolding and aggregation of the mutant AAT (ZAAT) in the endoplasmic reticulum (ER) of hepatocytes.^[5] Reduced AAT levels in circulation make individuals with AATD susceptible to lung issues, while hepatic accumulation of ZAAT polymers leads to liver disease through a toxic gain-of-function mechanism.^[6] ER stress, lipid droplet accumulation, mitochondrial dysfunction, and hepatocyte injury are thought to be primary causes of AATD-mediated liver disease.^[7–10]

Proteasomal degradation, lysosomal degradation, and autophagy are 3 major protein degradation pathways. The proteasome is responsible for the degradation of ~90% of misfolded AAT while ZAAT polymers are targeted for degradation by autophagy.^[11] Autophagy is a highly regulated mechanism involving the degradation of abnormal proteins by the autophagosome to be reutilized by the cell.^[12] Chaperone-mediated autophagy (CMA) is a form of autophagy in which cytosolic chaperones such as HSC70 facilitate selective uptake of misfolded proteins through lysosomal membrane receptor LAMP-2a.^[13,14] CMA also includes lipophagy wherein lipid droplets can be degraded through CMA. During lipophagy, lipid droplets containing fat are being transferred to the lysosomal pathway and undergo autophagic degradation.^[15] Sirtuin3 (SIRT3), a member of the sirtuins family, is a positive regulator of both CMA and lipophagy and is highly expressed in the liver.^[16,17] Mitochondrial SIRT3 is a NAD⁺-dependent protein deacetylase that maintains cellular homeostasis. SIRT3 regulates the activity of many mitochondrial proteins, modulating mitochondrial biogenesis and reactive oxygen species homeostasis. In the liver, SIRT3 regulates redox status and lipid homeostasis. Furthermore, SIRT3 plays an important role in cellular protection under pathological conditions such as ER stress.^[18]

In this study, utilizing ZAAT-expressing hepatocytes (HuhZ) and a novel AATD mouse model, we offer evidence of SIRT3's engagement in ZAAT quality control. We establish connections between hepatic ZAAT and lipid droplets, alongside disrupted SIRT3 function within AATD model systems. Notably, we identify ZAAT polymers interacting with lipid droplets through interaction with Perilipin2 (PLIN2), a lipid droplet surface marker. Our findings demonstrate that elevating SIRT3 levels mitigates both ZAAT and lipid accumulation in an AATD cell culture model. This is achieved by triggering lipophagy through SIRT3, which facilitates the clearance of lipid droplets and associated misfolded ZAAT. Further research on the mechanisms of lipophagy would reveal valuable new therapeutic targets including participants and regulators involved in lipophagy under physiological and pathological conditions and ultimately provide therapeutic approaches.

METHODS

Human subjects

The study protocols were approved by the Clinical Research Ethics Committee of the University of Florida (IRB202101148 and IRB201700650) and written consent was obtained from subjects in accordance with the Declaration of Helsinki Principles.^[19] A total of 17 AATD and age-matched and sex-matched healthy individuals (n=20) from the Alpha-1, and Liver DNA and Tissue Bank were enrolled in our study. The diagnosis of individuals with AATD was based on AAT genotyping and AAT serum level measurement using nephelometry (Behring Diagnostics). Fifty-three percent of individuals with AATD were on AAT augmentation therapy (60 mg of AAT/kg/wk). Plasma samples were obtained from individuals with AATD and healthy controls. A lung function test (FEV₁) on individuals with AATD has been also performed at the University of Florida. Detailed clinical data of all study subjects are shown in [Table 1](#).

Extracellular vesicle isolation

Plasma extracellular vesicles (EVs) were isolated through differential centrifugation, as we previously have shown.^[20] For detailed information, refer to SDC,

TABLE 1 Human plasma extracellular vesicle study patient demographics

	Subjects	
	Genotype MM (n = 20)	Genotype ZZ (n = 17)
Age (y)	52 (37–79)	59 (35–70)
Sex (female %)	60	59
FEV ₁ (%)	NA	68
AAT (μM)	27.2	≈5.2
Augmentation (%)	NA	53 (n=9)

Demographics of patients with AATD and healthy controls enrolled in the study. Abbreviations: AAT, alpha-1 antitrypsin; AATD, alpha-1 antitrypsin deficiency.

Materials and Methods, Supplemental Materials, <http://links.lww.com/HC9/A769>.

EV RNA isolation and library preparation

RNAs from EV were isolated using exoRNeasy Maxi Kit (Qiagen) and quantity and quality were determined using Agilent Bioanalyzer. For detailed information on library preparation methods, refer to SDC, Materials and Methods, Supplemental Materials, <http://links.lww.com/HC9/A769>.

Bioinformatics and functional pathway and network analyses

For detailed information on bioinformatics and functional pathway and network analyses, refer to SDC, Materials and Methods, Supplemental Materials, <http://links.lww.com/HC9/A769>.

Antibodies and reagents

For detailed information on antibodies and reagents, refer to SDC, Materials and Methods, Supplemental Materials, <http://links.lww.com/HC9/A769>.

Cell culture and transient transfection

HuhZ was previously generated using the CRISPR-Cas9 method inserting the Z variant of the *SERPINA1* gene into the AAT-knockout Huh7.5 cell line.^[21,22] Huh7.5 cell line was used as control (HuhM). Cells were cultured in DMEM containing 1% penicillin-streptomycin and 10% fetal bovine serum at 37°C and 5% CO₂. To overexpress SIRT3, cells were transiently transfected with SIRT3 plasmid using Xtreme Gene-HP. SIRT3 plasmid was cloned in-house.^[23]

Transgenic AATD mouse model

This study was performed with approval from the University of Florida Institutional Animal Care and Use Committee (IACUC no. 202300000056) with adherence to the Guide for Care and Use of Laboratory Animals (NIH, 86-23). Transgenic mice were produced by microinjection of the listed sequence into the oocytes of C57BL/6J-Serpina1 knockout mice (Strain #:035015).^[24] Transgenic mice express either the human wildtype (WT) (Pi*M) or mutant (Pi*Z) variant of AAT full DNA (Genbank ID: NC_000014.9; sequence 94374747 to 94395692) which contains both the macrophage and hepatocyte enhancer-promoter regions. Transgenic mice homozygous for human AAT transgene and their WT littermates (C57B6/J) were bred and maintained under pathogen-free conditions at 22 ± 3°C with a 12:12 h light-dark cycle and fed normal rodent chow.^[25] Mice were 3–4 months or 12 months old at the time of sacrifice and sex was not accounted for in the study due to lack of sex differences observed in AATD.

Immunohistochemistry

PI*Z and PI*M livers were formalin-fixed paraffin-embedded or embedded in optimal cutting temperature after 4% paraformaldehyde fixation and 30% sucrose cryopreservation. Tissues were sent to the University of Florida's Molecular Pathology Core (RRID: SCR_016601) for slicing and staining. For detailed information, refer to SDC, Materials and Methods, Supplemental Materials, <http://links.lww.com/HC9/A769>.

Western blotting and immunoprecipitation

Whole-cell lysates were collected using immunoprecipitation (IP) lysis buffer [0.025 M tris (pH = 7.5), 0.15 M NaCl, 1.0 M EDTA, 1% NP-40, and 5% glycerol] containing phosphatase and protease inhibitors and phenylmethyl sulfonyl fluoride, pelleted at 14,000 rpm, and postnuclear supernatant was collected. Protein concentrations were quantified by Bicinchoninic acid, prepared in denaturing conditions, and analyzed on a 4%–20% gradient tris-glycine gel. The gel was then transferred to a 0.45 μm nitrocellulose membrane. After blocking, the membranes were incubated with primary antibody overnight at 4°C. Membranes were probed using an Horseradish peroxidase-conjugated secondary antibody for 1 hour and imaged on a Bio-Rad imager using a chemiluminescent substrate. Postnuclear supernatant and Dyna-beads were utilized for co-IP (SDC, Materials and Methods, Supplemental Materials, <http://links.lww.com/HC9/A769>).

Cell fractionation

Cells were lysed in the isotonic-hypotonic buffer to retain cellular organelles along with phosphatase and protease inhibitors. Iodixanol gradients were prepared from a 60% stock iodixanol, diluted in isotonic buffer (2.5%, 5%, 7.5%, 10%, 15%, 17.5%, 20%, 25%, 30%, and 35%). The gradient was syringed by layering the lightest fraction at the bottom of a 14-mL ultracentrifuge tube and layering subsequent fractions underneath. Postnuclear supernatant was layered at the top and ultracentrifuged at 120,000 *g* for 1 hour at 4°C. Nine fractions were collected and analyzed by western blotting.

Immunostaining and immunofluorescent microscopy

Cells were seeded in 8-chambered slides and transiently transfected as previously described, for immunostaining to further analyzed by immunofluorescent microscopy (SDC, Materials and Methods, Supplemental Materials, <http://links.lww.com/HC9/A769>).

Confocal microscopy image acquisition and analysis

Confocal images were acquired on the Leica TCS SP5 confocal microscope at the University of Florida Cytometry Core (ICBR Cytometry Core Facility). In brief, 405, 543, and 633 nm lasers were used to image Hoechst, TRITC, and Cy5, respectively. Detectors gain and offset and laser power were defined using the brightest sample for each respective stain then remained consistent for all samples. Samples were imaged with a x63 water immersion at x3 zoom. Images were taken as a z-stack utilizing 0.13 μm Z-steps and compressed into a max compression projection image. Postimage processing was done using ImageJ and Adobe Photoshop.

Quantitative real-time PCR

Total RNA from cells or liver tissues was used for PCR assay. For detailed information, refer to SDC, Materials and Methods, Supplemental Materials, <http://links.lww.com/HC9/A769>.

Ultrastructure study of human liver explant

Explanted human liver tissue was processed and imaged at the University of Florida ICBR Electron Microscopy Core Facility. For transmission electron microscopy (TEM), pieces of human liver explant were fixed in 4% paraformaldehyde and 2.5% glutaraldehyde. Dehydrated

samples were infiltrated in anhydrous acetone-Spurr's epoxy resin with Z6040 embedding primer (Electron Microscopy Sciences) and semi-thick sections were collected. Prefixed tissues were then trimmed and immunogold labeling was performed using polyclonal rabbit anti-AAT antibody (Dako) at 1:10 dilution. Ultrathin sections were examined with a FEI Tecnai G2 Spirit Twin TEM (FEI Corp.) operated at 120 kV and digital images were acquired with a Gatan UltraScan 2kx2k camera and Digital Micrograph software (Gatan Inc.).

Statistical analysis

All results are expressed as means \pm SD. Statistical analyses were performed using Prism 9 software (GraphPad Software) by Student *t* test or Mann-Whitney *U* test. Values of $p < 0.05$ were considered statistically significant. For small RNA-sequencing data, FDR-adjusted $p < 0.05$ was also considered significant. For some genes of interest, the nonadjusted *p* value was also reported although the FDR-adjusted *p* value was not significant to reduce the type II error rate.^[26]

RESULTS

Plasma circulating mitochondrial RNA-sequencing reveals dysregulation of the SIRT3 pathway in individuals with AATD

TEM analysis of explanted liver tissue from an AATD individual showed megamitochondria formation in AATD liver tissue (Figure 1A) which is consistent with previous reports of mitochondrial dysfunction associated with AATD.^[21] To further confirm mitochondrial dysfunction in individuals with AATD, we performed small RNA-sequencing on plasma EV from healthy individuals ($n = 20$) and individuals with AATD ($n = 17$) (Table 1). We observed that AATD plasma EVs are significantly enriched with mitochondrial RNAs (mt-RNAs) compared to the plasma EV of healthy individuals (Figure 1B). A total of 13 mitochondrial mRNAs, 17 tRNAs, and 2 rRNAs were detected in the EV fraction of study subjects. Among them, we observed 7 dysregulated mt-RNAs in plasma EV of individuals with AATD as compared to healthy controls (Table 2). Upstream regulators of these dysregulated genes are listed in Supplemental Table S1, <http://links.lww.com/HC9/A770>. The dysregulated genes were further subjected to core pathway analyses using Ingenuity Pathway Analysis software. We performed an extensive comparison of functional enrichment and gene networks for mt-RNAs from plasma EV of control and individuals with AATD to further investigate molecular similarities/differences among the study groups. We observed that mt-RNAs related to mitochondrial dysfunction and oxidative phosphorylation were significantly upregulated in individuals with AATD.

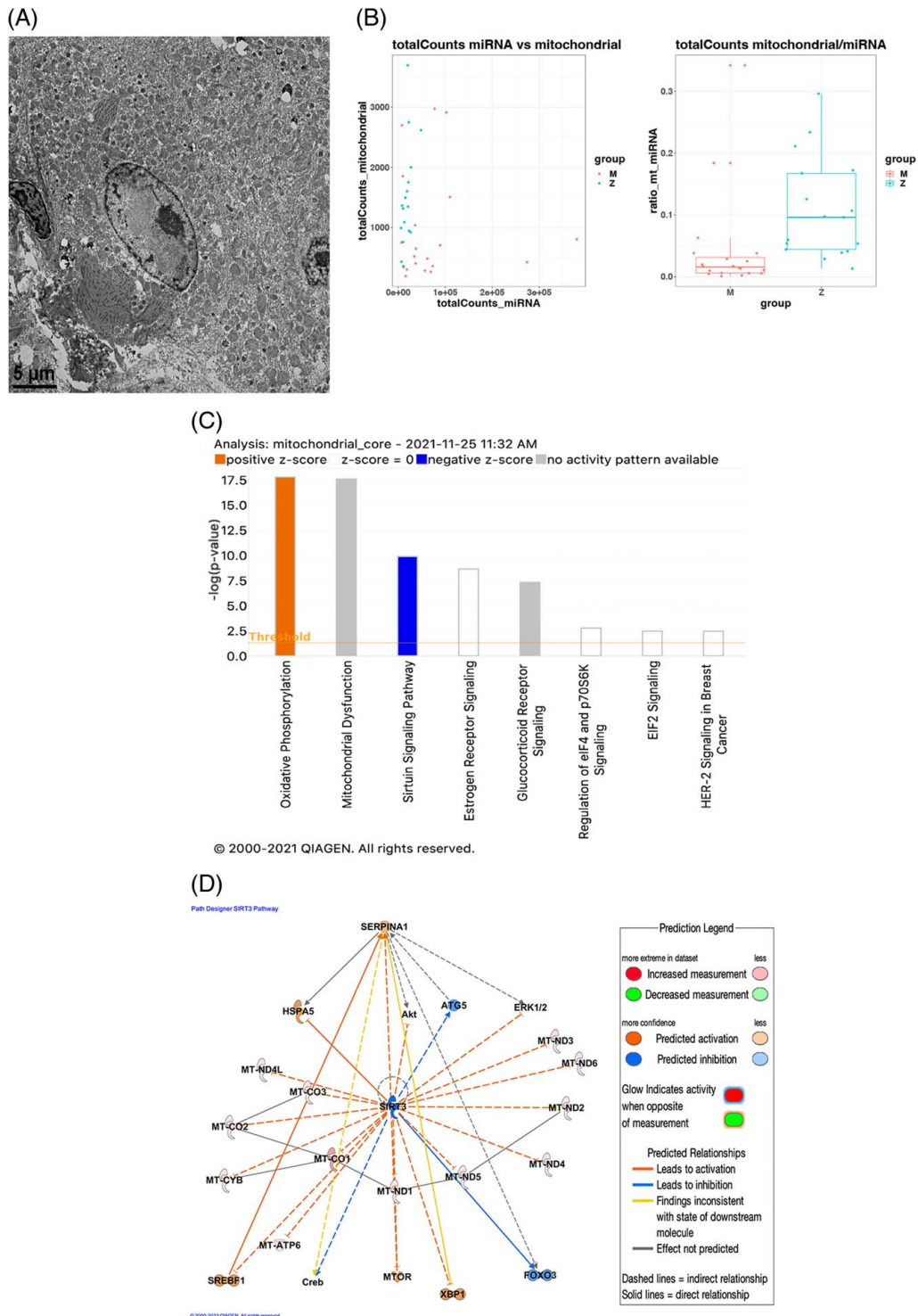


FIGURE 1 Mitochondrial RNA-sequencing reveals a link between SIRT3 protein and AATD. (A) Human AATD explanted liver tissue displaying megamitochondria. Images were taken with an FEI Tecnai G2 Spirit Twin TEM operated at 120 kV and digital images were acquired with a Gatan UltraScan 2kx2k camera and Digital Micrograph software. (B) PCA bar graph indicating the high abundance of mitochondrial RNA in plasma circulating extracellular vesicles from individuals with AATD ($n = 17$) as compared to healthy controls ($n = 20$). (C) Significantly upregulated and downregulated pathways as predicted by Ingenuity Pathway Analysis by Qiagen. Orange bars indicate a positive z-score and are predicted to be significantly upregulated while blue bars indicate a negative z-score and are predicted to be significantly downregulated. White bars indicate a z-score of zero while gray bars indicate no activity patterns. (D) Predicted SIRT3 pathway generated with Ingenuity Pathway Analysis. Green and red shading of proteins show increased or decreased expression levels, respectively, from the mt-RNA-sequencing data set. Orange shading indicates predicted activation and blue shading indicates predicted inhibition. The network is displayed with the subcellular localization of proteins and the software was told to connect SERPINA1 (AAT) and SIRT3 pathways. Solid lines are indicative of direct relationships and dashed lines are an indirect relationship. Abbreviations: AAT, alpha-1 antitrypsin; AATD, alpha-1 antitrypsin deficiency; PCA, Principal component analysis; SERPINA1, serpin family A member 1; SIRT3, Sirtuin3; TEM, transmission electron microscopy.

TABLE 2 Significant differentially expressed mitochondrial RNAs from alpha-1 antitrypsin deficiency patient plasma extracellular vesicles

mt-RNA	mean exp_M	mean Exp_Z	group MeanDiff	p
MT-CO1	4872.7431	15,044.5610	10,171.8179	0.007769
MT-TI	14.3658	0	-14.3658	0.008842
MT-CO2	2272.3626	5099.2286	2826.8660	0.02439
MT-TV	1.9488	30.8163	28.8675	0.02664
MT-ND5	446.1329	1015.4369	569.3040	0.02761
MT-ND3	921.5383	1929.2136	1007.6753	0.04481
MT-ND6	1137.02135	2646.4705	1509.4491	0.04987

List of 7 significant differentially expressed mt-RNAs in individuals with AATD plasma EV.
Abbreviations: AATD, alpha-1 antitrypsin deficiency; mt-RNA, mitochondrial RNA.

Significantly altered pathways included the sirtuin signaling pathway (Figure 1C), which was downregulated in individuals with AATD (Figure 1D). Biological functions associated with dysregulated mt-RNAs in individuals with AATD are illustrated in Figure 1B. SIRT3 has been predicted as a significantly inhibited upstream regulator in individuals with AATD (Figure 1D).

HuhZ cells have altered SIRT3 protein expression, cellular localization, and different lipid content

Our plasma EV-associated mt-RNA-sequencing results identified SIRT3 as a significantly dysregulated pathway in individuals with AATD. Therefore, we recruited HuhM and HuhZ cell lines to investigate RNA and protein expression levels of SIRT3, *in vitro*. While qPCR analysis showed no significant differences between RNA expression levels between groups (Figure 2A), western blot analysis showed reduced protein levels of full-length SIRT3 in HuhZ cells compared to HuhM (Figures 2B, C). Next, we performed immunofluorescence (IF) to investigate the subcellular localization of SIRT3 and observed that SIRT3 (green) colocalizes with mitochondrial marker TOM40 (red) in HuhM and to a lesser degree HuhZ cells (Figures 2D, E). To assess the lipid profile of HuhM and HuhZ cells, we subjected the cells to a neutral lipid stain to visualize lipid accumulation by immunofluorescent microscopy. We observed a large increase in the lipid content of HuhZ compared to HuhM control cells (Figure 2F). These findings demonstrate that HuhZ cells have altered SIRT3 protein expression and cellular localization as well as lipid profile compared to control hepatocytes.

Overexpression of SIRT3 reduces intracellular ZAAT accumulation in HuhZ cells independent of proteasomal or lysosomal degradation

SIRT3 has been shown to modulate proteins related to quality control signaling.^[16,17] To investigate whether SIRT3

plays a role in regulating ZAAT quality control, we transiently transfected HuhZ cells with 0.5 µg/mL of SIRT3 plasmid.^[23] Forty-eight hours after transfection, we observed high levels of mitochondrial SIRT3 (28 kDa) in SIRT3-transfected cells, indicating the presence of an active form of SIRT3. Interestingly, we found a significant reduction in intracellular ZAAT in the presence of SIRT3 plasmid and consequently a small decrease in extracellular ZAAT levels (Figures 3A, B). More ZAAT reduction was also observed in the treatment with a higher dose of the SIRT3 plasmid (Figure 3C). Next, we performed density gradient isolation of cellular proteins to qualitatively characterize ZAAT subcellular distribution and localization when SIRT3 is overexpressed (Figure 3D). Treatment with SIRT3 plasmid resulted in the migration of intracellular ZAAT to lighter fractions (fractions 4 and 5). Calnexin also migrated from the ER to the lighter-density fraction upon the increase of SIRT3 expression. This light-density fraction expresses LAMP1, an established marker for lysosomal and autophagolysosomal vesicles.^[27] We also observed colocalization of ZAAT and HSC70 in the presence of SIRT3. Furthermore, SIRT3 in the transfected cells colocalized with mitochondrial markers, TOM20 and TOM40, indicating the association of the overexpressed SIRT3 with mitochondria. In addition, there was an increase in the expression of LAMP1, a well-established autophagy-related protein, in SIRT3-transfected cells compared to control cells. These results demonstrate that overexpression of SIRT3 resulted in the localization of ZAAT with lighter fractions localized with autophagosome markers as well as increased expression of autophagy-related proteins (Figure 3D). To further demonstrate that overexpressed SIRT3 is localized in the mitochondria, we subjected HuhZ cells, with and without SIRT3 overexpression, to IF and observed that overexpressed SIRT3 (green) colocalized with TOM40 (red) in transfected cells compared to control cells in which SIRT3 mainly localizes in the nucleus (Figure 3E).

To further identify the mechanism of SIRT3-mediated reduction of hepatic ZAAT in HuhZ cells, we inhibited 2 major degradation pathways using MG-132, an inhibitor of the proteasomal degradation pathway, and Bafilomycin A1 (BafA1), a lysosomal degradation inhibitor, in HuhZ

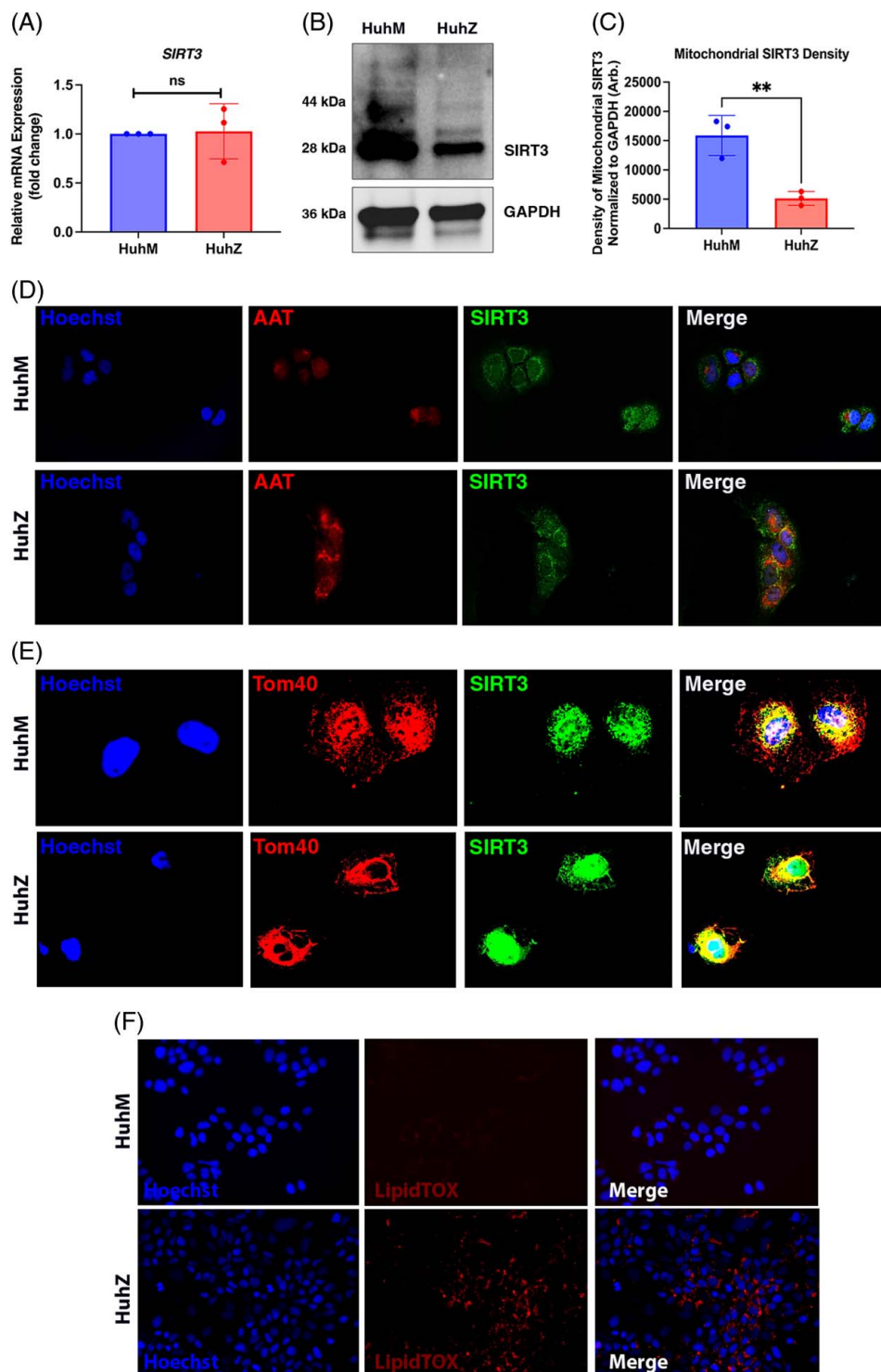


FIGURE 2 SIRT3 protein levels are downregulated and have a different cellular localization in Z AAT versus MAAT-expressing human hepatocytes. (A) qPCR data showing SIRT3 expression differences between M and Z cells. SIRT3 mRNA was normalized to housekeeping gene 18S. Data displayed as fold changes compared with control samples. Statistical analysis by Mann-Whitney *U* test ($n = 3$). (B) Western blot depicting the differences in SIRT3 protein expression level in HuhM and HuhZ cells. GAPDH was used as a loading control. (C) Densitometry analysis of mitochondrial SIRT3 (28 kDa) protein expression normalized to GAPDH ($n = 3$). (D) Representative immunofluorescent microscopy images at $\times 40$ of polymerized AAT (red) and SIRT3 (green) and Hoechst (blue) counterstain in HuhM and HuhZ cells showing the cellular distribution of SIRT3 and abundance of polymerized AAT. (E) Representative immunofluorescent microscopy images at $\times 40$ of SIRT3 (green) and TOM40 (red) and Hoechst (blue) counterstain in HuhM and HuhZ cells showing the differential distribution of SIRT3 and the colocalization of SIRT3 in the mitochondria of HuhM cells and nuclear colocalization of SIRT3 in HuhZ cells. (F) Representative immunofluorescent microscopy staining at $\times 40$ of LipidTOX staining in HuhM and HuhZ cells with Hoechst counter stain. Abbreviations: AAT, alpha-1 antitrypsin; GAPDH, glyceraldehyde 3-phosphate dehydrogenase; n.s., nonsignificant; qPCR, quantitative polymerase chain reaction; SIRT3, Sirtuin3; TOM40, translocase of outer mitochondrial membrane 40 homolog. * $p < 0.05$, ** $p < 0.01$, *** $p < 0.001$, **** $p < 0.0001$.

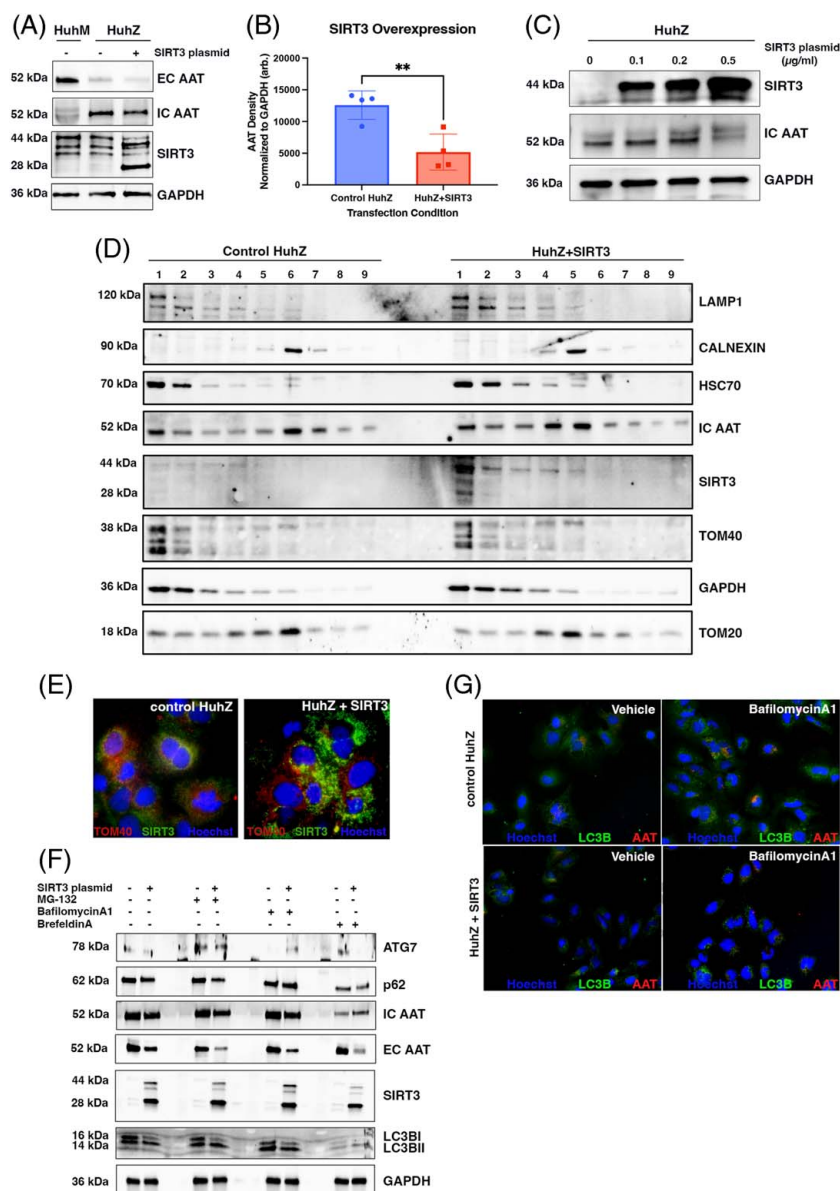


FIGURE 3 Overexpression of SIRT3 reduces intracellular ZAAT accumulation in HuhZ cells, independent of proteasomal or lysosomal degradation. (A) Western blot depicting overexpression of SIRT3 in HuhZ cells reduces intracellular AAT compared to control cells (HuhZ+empty vector) with HuhM cells acting as a healthy control. Markers include EC/IC AAT and SIRT3 with GAPDH as a loading control. SIRT3 plasmid was transfected at a concentration of 0.5 µg/mL as determined from dose-response results in (C). (B) AAT density measured by densitometry using ImageJ software shows that SIRT3 overexpression significantly reduces intracellular AAT compared to empty vector-transfected cells ($n = 4$). Statistical analysis by unpaired t test. (C) Western blot showing SIRT3 overexpression reduces intracellular AAT, dose-dependently. Markers shown are IC AAT and SIRT3, with GAPDH as a loading control. (D) Western blot depicting density gradient cell fractionation of HuhZ cells with and without overexpression of SIRT3. Markers include LAMP1, Calnexin, HSC70, IC AAT, SIRT3, TOM40, GAPDH, and TOM20. Cell fractionation shows the distribution of SIRT3 in transfected cells and changes to intracellular markers under SIRT3 overexpression ($n = 1$). (E) Representative immunofluorescent images at $\times 100$ of control HuhZ cells and HuhZ under SIRT3 overexpression. Markers are TOM40 (red) and SIRT3 (green) and counterstained with Hoechst (blue). Images depict the subcellular localization of SIRT3 in control and overexpressed cells ($n = 1$). (F) Western blot of HuhZ and SIRT3 overexpression when treated with MG-132, a selective proteasomal inhibitor, Bafilomycin A1, a proton pump inhibitor, or Brefeldin A, an inhibitor of ER to Golgi vesicular transport ($n = 1$ per treatment group). Markers include SIRT3, IC AAT, EC AAT, ATG7, p62, and LC3BI/II, with GAPDH as a loading control. With each inhibition, the SIRT3-mediated decrease in intracellular AAT was unaffected. (G) Representative immunofluorescence microscopy at $\times 40$ of treatment of HuhZ cells when treated with Bafilomycin A1 and staining for LC3B (green) and polymerized AAT (red) and counterstained with Hoechst (blue). Consistent with western blots, the decrease in accumulated AAT was unaffected by the inhibition with Bafilomycin A1. Abbreviations: AAT, alpha-1 Antitrypsin; EC, extracellular; GAPDH, glyceraldehyde 3-phosphate dehydrogenase; HSC70, heat shock cognate 71 kDa protein; IC, intracellular; LAMP1, lysosomal association membrane protein 1; n.s., nonsignificant; SIRT3, Sirtuin3; TOM20, translocase of outer mitochondrial membrane 20 homolog; TOM40, translocase of outer mitochondrial membrane 40 homolog. * $p < 0.05$, ** $p < 0.01$, *** $p < 0.001$, **** $p < 0.0001$.

control cells and cells transfected with SIRT3 plasmid. To assess the probable effect of SIRT3 on Golgi transport, Brefeldin A, an ER to Golgi anterograde transport inhibitor, has been used as well. The results indicated that SIRT3-mediated reduction of intracellular ZAAT is not restored when SIRT3 overexpressing cells were treated with either inhibitor. This suggests that SIRT3 is acting independently of proteasome or autophagy degradation pathways, inducing degradation of ZAAT in HuhZ cells (Figure 3F). However, HuhZ cells overexpressing SIRT3 when inhibited by BafA1, ATG7, a key autophagy protein, was still present, leading us to hypothesize autophagy is not fully inhibited (Figure 3F). In addition, ATG7 is essential for lipophagy in the liver.^[15] To identify whether autophagy was still active even in the presence of BafA1, we treated the overexpressed SIRT3 HuhZ cells with 100 μ M of BafA1 and then subjected the cells to IF microscopy to visualize if autophagy was active through LC3B (Figure 3G). When treated with BafA1, there was an accumulation of LC3B puncta (green), indicating an increase of autophagosomes due to the loss of autophagosome/lysosome fusion events. Interestingly, there is no increase in accumulated AAT (red) levels after treatment with BafA1 in the SIRT3-transfected cells, leading us to hypothesize that SIRT3-mediated AAT degradation is independent of the classical macroautophagy pathway.

SIRT3 overexpression results in degradation of ZAAT through lipophagy

Considering the regulatory role of SIRT3 in the activation of lipophagy, we investigated if overexpression of SIRT3 in HuhZ cells can clear lipid accumulation associated with AATD in vitro.^[28] We subjected control HuhZ cells and cells transfected with SIRT3 plasmid to a neutral lipid stain and observed that SIRT3 overexpression significantly reduces lipid accumulation associated with AATD phenotype (Figures 4A, B).^[28] It has been demonstrated that lipid droplets can disintegrate with misfolded proteins associated with them.^[15] Our IF staining for PLIN2, a lipid droplet coating protein and AAT polymers confirmed that ZAAT polymers colocalize with PLIN2 on the surface of lipid droplets in HuhZ cells (Figure 4C).^[29] Interestingly, when HuhZ cells were transfected with SIRT3, there was a reduction in the size of PLIN2-positive lipid droplets (yellow) as well as reduction in intracellular levels of AAT (red) as previously shown (Figure 4C). To assess if ZAAT polymers associate with lipid droplets in AATD hepatocytes, we subjected an explanted AATD human liver tissue to TEM. Immunogold-positive AAT staining revealed that AAT aggregates were associated with lipid droplets in AATD liver tissue (Figure 4D). In addition, we observed that although less AAT was detected in SIRT3-transfected HuhZ cells, co-IP

analysis indicated slightly elevated levels of PLIN2 associated with AAT in those cells (Figures 4E, F). Next, to investigate the activation of CMA involving HSC70 chaperone, we performed co-IP experiments and observed lower levels of PLIN2 in association with HSC70 in HuhZ cells that overexpress SIRT3 compared to control HuhZ (Figures 4G, H).^[15] However, due to diverse backgrounds in the various blots, achieving perfect matching in band intensity quantification is challenging. As a result, the significance of 3 replicates may not be conclusive initially, but there was a trend toward significance. The low levels of PLIN2 associated with HSC70 in the presence of SIRT3 are consistent with the hypothesis that lipid droplets are being cleared with ZAAT and thus fewer PLIN2-positive lipid droplets are detected in association with HSC70. In agreement with the activation of lipophagy in SIRT3 overexpressing cells, our IF analysis showed colocalization of HSC70 (green) with LAMP2 (red) in SIRT3-transfected HuhZ cells (Figure 4I).

Humanized AATD transgenic mice have lower hepatic SIRT3 expression along with hepatic accumulation of ZAAT polymers and lipid droplets

We have generated a novel humanized transgenic mouse model of AATD by inserting the human WT (MAAT) or mutated (ZAAT) *SERPINA1* transgene into a C57BL/6J-Serpina1 knockout mouse (Null mice, Jax Labs Strain #: 035015). While body weight had no observed differences between WT (Pi*M) and mutant (Pi*Z) transgenic mice (data not shown), consistent with liver accumulation of AAT in human AATD, Pi*Z mice display ZAAT globules in the liver as determined by PAS-D^[30,31] (Figure 5A). However, Pi*M livers were negative for PASD staining, consistent with normal liver histopathology (Figure 5A).^[32] Plasma levels of human AAT measured by nephelometry are also lower in Pi*Z mice with an average of 10 μ M compared to Pi*M which were around 30 μ M and within the physiologically relevant range for human subjects (Figure 5B).^[33] Furthermore, Oil-Red-O staining demonstrated increased lipid droplets in the liver of Pi*Z compared to Pi*M mice (Supplemental Figure S1, <http://links.lww.com/HC9/A771>) indicating that AATD transgenic mice recapitulate human AATD liver pathophysiology.

To assess the expression of Sirt3 in the liver tissue of AATD mice, Pi*M and Pi*Z livers were subjected to protein analysis by western blotting, which confirmed the upregulation of Sirt3 protein levels (Figures 5C, D). Interestingly, proteolytically cleaved Sirt3 representative of active, mitochondrial Sirt3, presented inversely correlated with levels of intracellular AAT (Figure 5E), consistent with our in vitro findings. Immunohistochemistry confirmed these findings, in which there was decreased

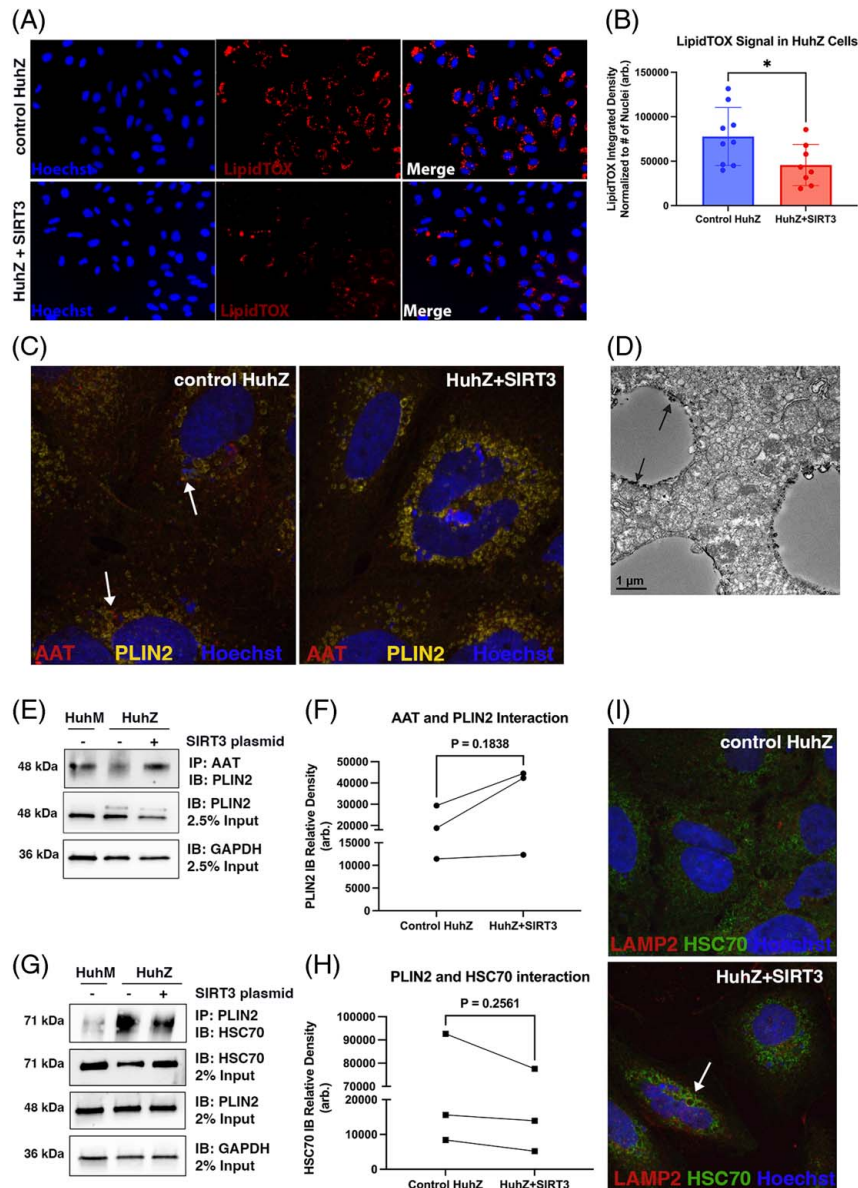


FIGURE 4 SIRT3 overexpression in ZAAT-expressing hepatocytes promotes the degradation of ZAAT through activation of lipophagy. (A) Representative immunofluorescent microscopy images at $\times 40$ of LipidTOX deep red neutral lipid stain (red) at 1:100 and counterstained with Hoechst (blue) in HuhM cells and HuhZ cells with and without SIRT3 overexpression. SIRT3-transfected cells show a decrease in lipid accumulation compared to empty vector-transfected control cells. (B) Quantification of LipidTOX images in (A). Images were quantified in ImageJ and data are represented as an integrated density of LipidTOX signal normalized to the number of nuclei in the field. Statistical analysis by unpaired *t* test. ($n = 8-9$). (C) Representative confocal immunofluorescent microscopy images of HuhZ cells at $\times 63$ water immersion staining for polymerized AAT (red) and PLIN2 (yellow) and counterstained with Hoechst (blue) in the absence and presence of SIRT3. Arrows indicate AAT associated with PLIN2 lipid droplets. The image displayed as a max compression from a z-stack taken at 0.13 μ m steps ($n = 1$). (D) Transmission electron microscopy images of AATD human explanted liver indicating association of immunogold-labeled AAT with lipid droplets. Images were taken with an FEI Tecnai G2 Spirit Twin TEM operated at 120 kV and digital images were acquired with a Gatan UltraScan 2k \times 2k camera and Digital Micrograph software. (E) Immunoprecipitation of AAT with 2.5% input. Immunoblots show PLIN2, AAT, HSC70, and GAPDH as loading control. (F) Quantification of AAT IP showing a pairwise increase of PLIN2 density in SIRT3 overexpressed cells compared to control cells. Statistical analysis by paired *t* test ($n = 3$). (G) Immunoprecipitation of PLIN2 with 2% input. Immunoblots show PLIN2, HSC70, and GAPDH as loading control. (H) Quantification of PLIN2 IP showing a pairwise decrease in SIRT3 overexpressed cells compared to control cells. Statistical analysis by paired *t* test ($n = 3$). (I) Representative confocal immunofluorescent microscopy images of HuhZ cells at $\times 63$ water immersion staining for LAMP2 (red) and hsc70 (green) and counterstained with Hoechst (blue). The image displayed as a max compression from a z-stack taken at 0.13 μ m steps ($n = 1$). Abbreviations: AAT, alpha-1 antitrypsin; EC, extracellular; GAPDH, glyceraldehyde 3-phosphate dehydrogenase; HSC70, heat shock cognate 71 kDa protein; IC, intracellular; LAMP2, lysosomal association membrane protein 2; n.s., nonsignificant; PLIN2, Perilipin2; SIRT3, Sirtuin3. * $p < 0.05$, ** $p < 0.01$, *** $p < 0.001$, **** $p < 0.0001$.

Sirt3 staining in the liver of Pi*Z compared to Pi*M mice (Figure 5F). However, consistent with our *in vitro* data the qPCR analysis showed no differences in mRNA levels of SIRT3 (Figure 5G). These data suggest that Sirt3 activity is dysregulated in our transgenic AATD mice consistent with our *in vitro* model.

DISCUSSION

In this present study, we investigated the impact of SIRT3 on maintaining the quality of hepatic ZAAT and lipids while also exploring whether upregulating SIRT3 expression can mitigate AATD-induced liver damage. Our study effectively establishes the presence of mitochondrial dysfunction due to AATD and reveals the dampened activity of SIRT3, both within individuals with AATD and AATD model systems. Furthermore, this discovery is confirmed by observing a negative correlation between SIRT3 expression and accumulation of ZAAT and lipids in AATD hepatocytes. Through our research, we demonstrated that elevating SIRT3 levels prompts the degradation of lipid droplets and ZAAT polymers, operating through a collaborative mechanism involving lipophagy (Figure 6). These findings align with earlier research that highlighted the role of lipophagy in the degradation of protein aggregates seen in metabolic disorders.^[15]

The close proximity of mitochondria, key organelles responsible for energy production, to the ER assumes significance in the context of liver diseases characterized by ER stress such as AATD.^[34] The ER and mitochondria physically associate through contact sites known as mitochondria-associated membranes (MAMs). These MAMs create a platform for direct communication between the 2 organelles.^[35] MAMs facilitate the protein exchange between the ER and mitochondria playing a crucial role in mediating the physical and functional interactions between the ER and mitochondria. MAMs also play a role in the exchange of lipids between the ER and mitochondria, and this includes interactions with lipid droplets.^[35] In this regard, we have previously shown that misfolded ZAAT enters the mitochondria recruiting cytoplasmic HSP70 leading to mitochondrial injury, which stimulates the release of mt-RNA into the cytoplasm.^[21,36] Secreted mt-RNA can be encapsulated into EV and released from cells.^[37] This has been proposed to serve as a form of quality control, participating in cellular metabolic regulation.^[38] By examining the plasma of individuals with AATD, we have observed elevated quantities of dysregulated mt-RNA associated with plasma EV. These findings highlight the prevalence of EV with altered content in the plasma of patients with AATD. Notably, the release of EV containing mt-RNA from cells exhibiting mitochondrial dysfunction holds the potential to serve as a mechanism for removing

mitochondrial material from compromised cells and alleviation of tissue injury.^[36] The high level of mt-RNA in AATD plasma EV is in line with the observation of mitochondrial dysfunction triggered by misfolded ZAAT.^[39] Furthermore, Ingenuity Pathway Analysis revealed oxidative phosphorylation and mitochondrial dysfunction were significantly enriched pathways in individuals with AATD. Oxidative phosphorylation constitutes the pathway in which ATP is produced through a sequence of redox reactions along the mitochondrial membrane. Anomalies in oxidative phosphorylation stand as the predominant trigger of mitochondrial dysfunction leading to metabolic disorders.^[40]

Pathway enrichment analysis from plasma EV mt-RNA–sequencing also revealed inhibition of the sirtuin signaling pathway in individuals with AATD. The role of SIRT3 in regulating cellular quality control led us to investigate whether SIRT3 plays a role in ZAAT quality control in hepatocytes.^[41] Observing the decreased SIRT3 protein levels in an AATD cell culture model, we hypothesized that elevating SIRT3 expression might lead to an augmentation in ZAAT degradation. Our findings revealed that the overexpression of SIRT3 results in a reduction of intracellular ZAAT levels in HuhZ cells, with the degree of reduction corresponding to the dose of SIRT3. Previous data have emphasized the role of SIRT3 in inducing lipophagy and regulating lipid metabolism in hepatocytes.^[28] While the accumulation of lipid droplets in the liver is also intertwined with the manifestation of the AATD,^[21] our lipid staining results similarly showed a decrease in lipid droplets within hepatocytes characterized by SIRT3 overexpression. This finding supports the understanding of SIRT3's significance in governing cellular pathways linked to the detrimental gain-of-function exhibited by ZAAT and AATD phenotypes. To shed light on this observation, we investigated the mechanisms that underlie SIRT3's role in reducing intracellular ZAAT levels and diminishing the lipid droplets in our AATD cell culture model.

Lipid droplets have been shown to be involved in the maintenance of cellular homeostasis through different pathways. In stressed cells, lipid droplets stay connected to the ER and respond to ER stress.^[42] It has been evidenced that lipid droplets remove misfolded proteins and also play roles in regulating autophagy.^[42] We have previously shown that the accumulation of ZAAT globules within hepatocytes impairs lipid metabolism pathways and increases the lipid content of AATD hepatocytes.^[21] Here, we have noted that ZAAT polymers associate with lipid droplets by interacting with PLIN2 within HuhZ cells. Conversely, there is an absence of interaction between MAAT and PLIN2 within HuhM cells.^[21] These data align with the concept of lipid droplets serving as protective reservoirs that sequester misfolded proteins, thus mitigating ER stress.^[43] SIRT3's known role in safeguarding hepatocytes from

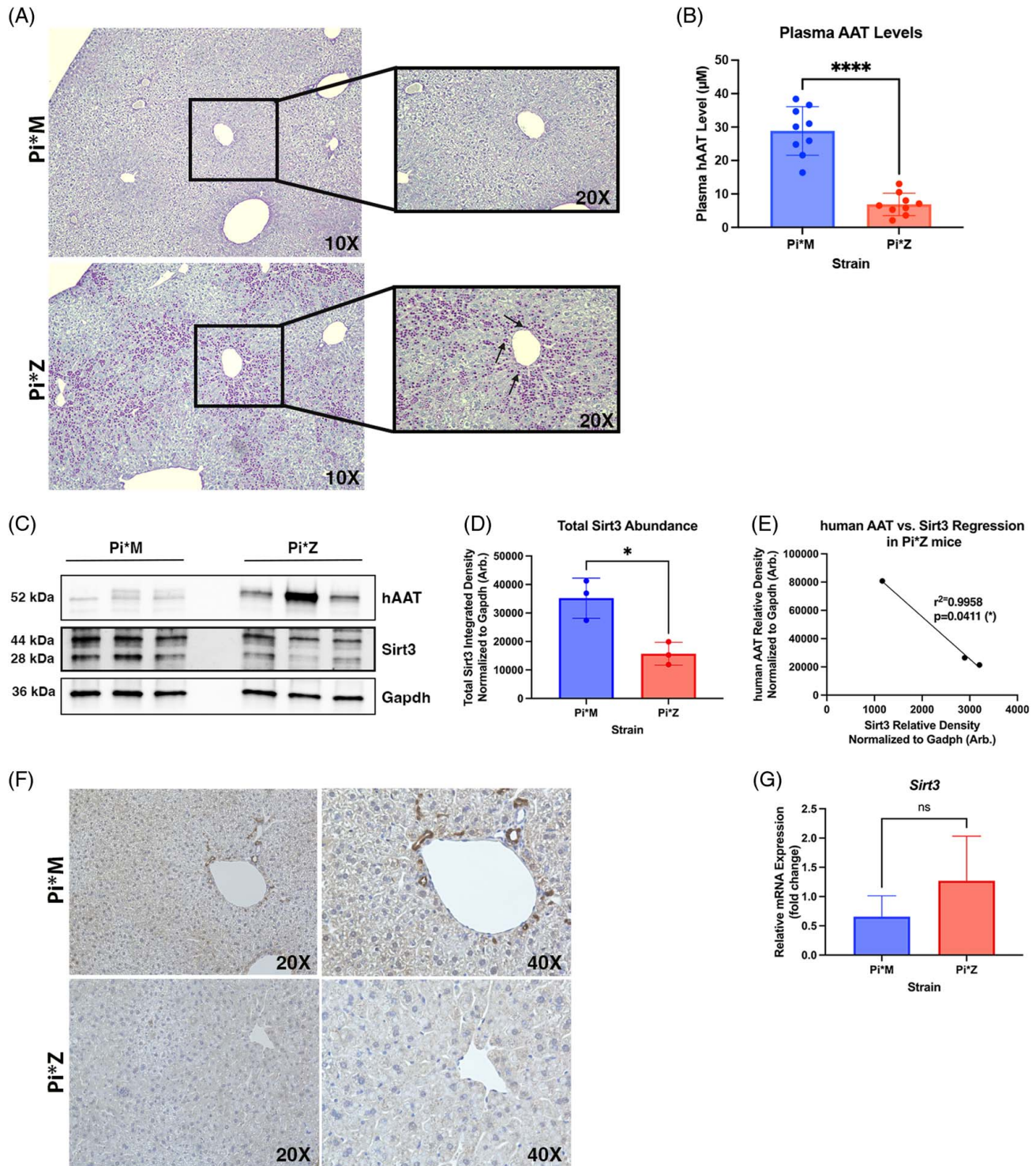


FIGURE 5 Characterization of the humanized MAAT and ZAAT mouse model. (A) Representative IHC microscopy at $\times 10$ of PAS-D staining of liver tissue collected from Pi*M and Pi*Z mice performed by the University of Florida Pathology core. The focused panel is at $\times 20$. The arrow indicates the PAS-D-positive AAT inclusion bodies ($n = 3$). (B) Plasma human AAT levels measured by Nephelometry. Statistical analysis by Mann-Whitney U test ($n = 6$). (C) Western blotting depicting differential protein expression of Sirt3 and intracellular human AAT with Gapdh as a loading control between Pi*M and Pi*Z mouse livers. (D) Total Sirt3 densitometry normalized to Gapdh between Pi*M and Pi*Z mice. Statistical test by unpaired t test ($n = 3$). (E) Linear regression analysis of mitochondria Sirt3 fraction (28 kDa) density and hAAT density ($n = 3$). (F) Representative IHC staining microscopy images at $\times 20$ and $\times 40$ of Sirt3 in Pi*M and Pi*Z liver tissues performed by the University of Florida Pathology core ($n = 3$). (G) qPCR data showing Sirt3 expression differences between Pi*M and Pi*Z liver tissues normalized to 18S housekeeping gene. Data displayed as fold changes compared with control samples. Statistical analysis by Mann-Whitney U test ($n = 3$). Abbreviations: AAT, alpha-1 antitrypsin; Gapdh, glyceraldehyde 3-phosphate dehydrogenase; IHC, immunohistochemistry; n.s., nonsignificant; qPCR: quantitative polymerase chain reaction; Sirt3, mouse Sirtuin3. * $p < 0.05$, ** $p < 0.01$, *** $p < 0.001$, **** $p < 0.0001$.

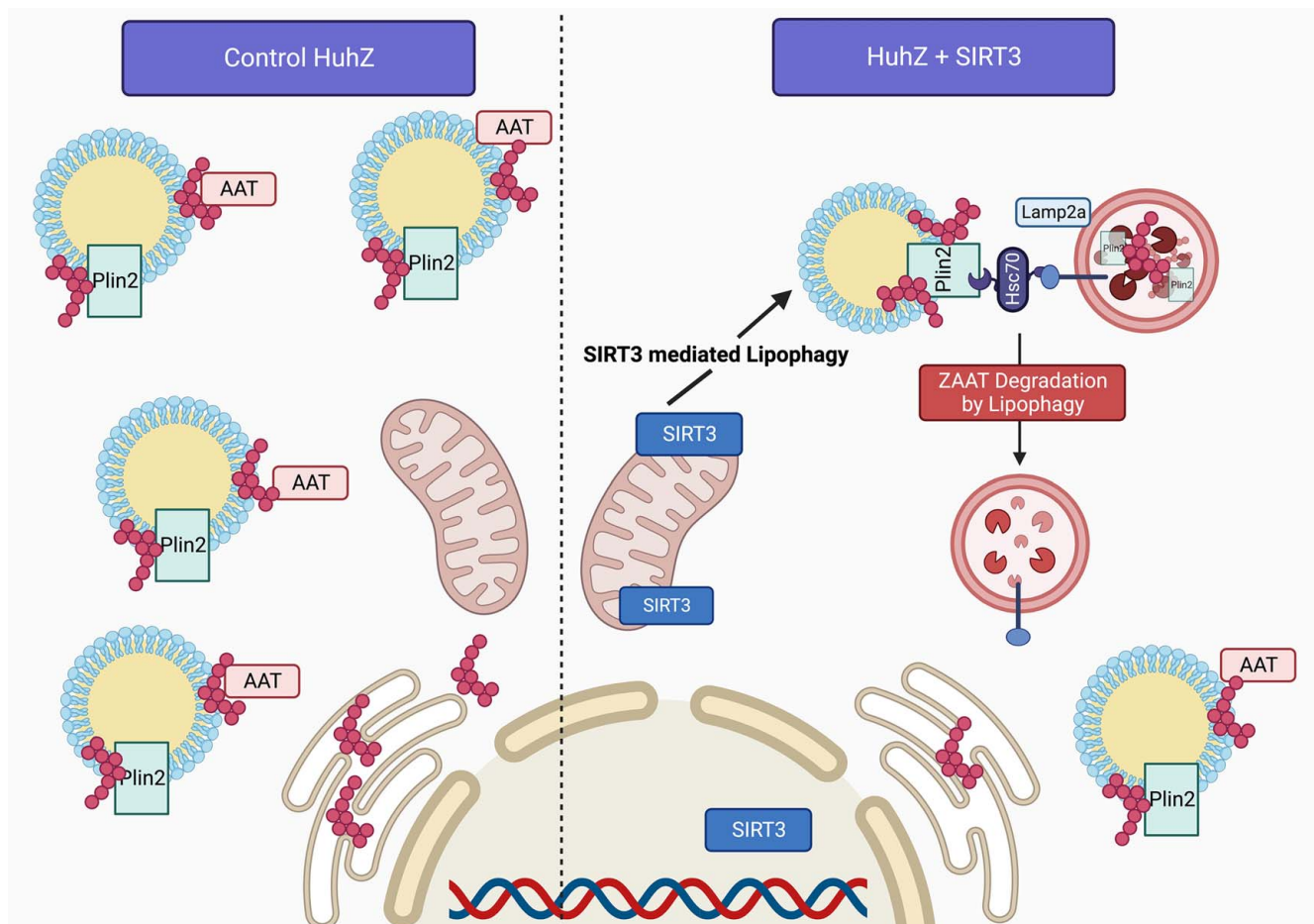


FIGURE 6 Graphical summary. Graphical schematic of the findings reported in this paper. HuhZ cells have an increased amount of polymerized ZAAT that is associated with PLIN2-coated lipid droplets. Under the overexpression of SIRT3, HuhZ cells clear polymerized AAT along with lipid droplets through SIRT3-mediated lipophagy. Abbreviations: AAT, alpha-1 antitrypsin; SIRT3, Sirtuin3.

lipotoxicity involves fostering processes like CMA and lipophagy.^[28] In the context of lipophagy, the degradation of lipid droplets hinges on the interaction between PLIN2 on their surface and the lysosome-HSC70 complex.^[15] Within this process, phospho-PLIN-2 interacts with HSC70 and associates with lysosomal LAMP2, consequently triggering CMA-mediated lipophagy.^[15] As a result, our hypothesis posited that SIRT3 facilitates the degradation of ZAAT together with lipid droplets through the mechanism of lipophagy. We observed a diminished presence of lipid droplets and PLIN2 in association with HSC70 within SIRT3-transfected HuhZ cells. This observation admits the advantageous regulatory role of SIRT3 in modulating lipophagy. Intriguingly, even though there is a reduction in polymeric AAT in SIRT3-transfected HuhZ cells, the AAT-PLIN2 complex remains detectable through co-IP. These findings support our proposition that ZAAT undergoes degradation alongside lipid droplets through the involvement of lipophagy and PLIN2. This also implies that SIRT3 promotes the degradation of lipid droplets and subsequently, the associated ZAAT polymers.

In conclusion, the data presented in this study unveil the engagement of mitochondrial SIRT3 in overseeing ZAAT quality within hepatocytes. Our findings demonstrate that mitochondrial SIRT3 activates the process of lipophagy, a mechanism that contributes to the breakdown of ZAAT aggregates linked with lipid droplets (Figure 6). This relationship between hepatic ZAAT and lipid droplets was also expounded upon in our study. The functional insights gathered lend support to the notion that the elevated expression of SIRT3 efficiently mobilizes the lipophagy degradation apparatus, facilitating the disposal of lipid droplets and consequently, ZAAT associated with them. Intriguingly, our investigations extended to a humanized AATD mouse model, revealing a disrupted regulation of SIRT3. Furthermore, a reciprocal correlation emerged between the abundance of SIRT3 protein and intracellular AAT levels. These findings underline that the augmentation of the lipophagy pathway through SIRT3 overexpression, coupled with the concurrent degradation of lipid droplet-associated ZAAT, significantly reduces the aggregation of ZAAT polymers in HuhZ cells.

The data above suggest a potential therapeutic avenue for AATD-associated liver disease. SIRT3

emerges as a promising target for drugs aimed at mitigating hepatic ZAAT and lipid droplets in AATD liver tissues. However, our study has limitations. The use of immortalized cell lines is a starting point, and validation through primary cells or in vivo models is further needed. Limited plasma EV-associated mt-RNA samples are another constraint. Due to AATD's rarity, obtaining large human cohorts for samples remains a challenge. Our findings set the stage for future in vivo studies probing SIRT3's viability in AATD liver treatment, considering its relevance in diverse liver diseases.^[44–47] Our future directives include identifying the mechanism of action of SIRT3-mediated degradation of misfolded ZAAT as well as using the humanized AATD mouse models to determine if our in vitro observations can be recapitulated in vivo.

AUTHOR CONTRIBUTIONS

Brittney Poole: investigation and writing—original draft, review, and editing. Regina Oshins: investigation, technical support, and writing—review and editing. Zhiguang Huo: data curation, formal analysis, and review and editing. Sergio Duarte: investigation and writing—review and editing. Jesse West: investigation. Ginger Clark: investigation. Mark Brantly: conceptualization and supervision. Nazli Khodayari: conceptualization, funding acquisition, formal analysis, data curation, supervision, and writing the original draft, review, and editing.

ACKNOWLEDGMENTS

The authors acknowledge the University of Florida's ICBR core technicians, Doug Smith (Cytometry Core, RRID: SCR_019146) and Rudy Alvarado (Electron Microscopy Core, RRID:SCR_019146) for their assistance in training and acquisition of microscopy images in this manuscript. They also thank the University of Florida ICBR NextGen DNA Sequencing Core Facility (RRID:SCR_019152) and University of Florida ICBR Gene Expression and Genotyping Core Facility (RRID:SCR_019145) for assistance in gene sequencing and gene expression analysis in the human studies. They also thank the University of Florida Molecular Pathology Core (RRID:SCR_016601) for sectioning and staining of liver tissues.

FUNDING INFORMATION

Financial support: Alpha-1 Foundation.

CONFLICTS OF INTEREST

Virginia Clark consults and received grants from Takeda. She received grants from Arrowhead, Vertex, and Hanmi. The remaining authors have no conflicts to report.

ORCID

Brittney Poole  <https://orcid.org/0000-0002-09558815>

Virginia C. Clark  <https://orcid.org/0000-0001-6719-3634>

REFERENCES

- Kokturk N, Khodayari N, Lascano J, Riley EL, Brantly ML. Lung inflammation in alpha-1-antitrypsin deficient individuals with normal lung function. *Respir Res.* 2023;24:40.
- Sifers RN. Intracellular processing of alpha1-antitrypsin. *Proc Am Thorac Soc.* 2010;7:376–80.
- Greene CM, Marciniak SJ, Teckman J, Ferrarotti I, Brantly ML, Lomas DA, et al. α 1-Antitrypsin deficiency. *Nat Rev Dis Primers.* 2016;2:16051.
- Seixas S, Marques PI. Known mutations at the cause of alpha-1 antitrypsin deficiency an updated overview of SERPINA1 variation spectrum. *Appl Clin Genet.* 2021;14:173–94.
- Ferrarotti I, Carroll TP, Ottaviani S, Fra AM, O'Brien G, Molloy K, et al. Identification and characterisation of eight novel SERPINA1 null mutations. *Orphanet J Rare Dis.* 2014;9:172.
- Hidvegi T, Mukherjee A, Ewing M, Kemp C, Perlmutter DH. The role of autophagy in alpha-1-antitrypsin deficiency. *Methods Enzymol.* 2011;499:33–54.
- Goeckeler JL, Brodsky JL. Molecular chaperones and substrate ubiquitination control the efficiency of endoplasmic reticulum-associated degradation. *Diabetes, Obes Metab.* 2010;12:32–8.
- Gelling CL, Brodsky JL. Mechanisms underlying the cellular clearance of antitrypsin Z: Lessons from yeast expression systems. *Proc Am Thorac Soc.* 2010;7:363–7.
- Ghouse R, Chu A, Wang Y, Perlmutter DH. Mysteries of α 1-antitrypsin deficiency: Emerging therapeutic strategies for a challenging disease. *Dis Model Mech.* 2014;7:411–9.
- Kroeger H, Miranda E, MacLeod I, Pérez J, Crowther DC, Marciniak SJ, et al. Endoplasmic reticulum-associated degradation (ERAD) and autophagy cooperate to degrade polymerogenic mutant serpins. *J Biol Chem.* 2009;284:22793–802.
- Marciniak SJ, Ordóñez A, Dickens JA, Chambers JE, Patel V, Dominicus CS, et al. New concepts in alpha-1 antitrypsin deficiency disease mechanisms. *Ann Am Thorac Soc.* 2016;13 (suppl 4S): 289–96.
- Klionsky DJ, Emr SD. Autophagy as a regulated pathway of cellular degradation. *Science.* 2000;290:1717–21.
- Orenstein SJ, Cuervo AM. Chaperone-mediated autophagy: Molecular mechanisms and physiological relevance. *Semin Cell Dev Biol.* 2010;21:719–26.
- Poljšak B, Milisav I. Clinical implications of cellular stress responses. *Bosn J Basic Med Sci.* 2012;12:122.
- Zhang S, Peng X, Yang S, Li X, Huang M, Wei S, et al. The regulation, function, and role of lipophagy, a form of selective autophagy, in metabolic disorders. *Cell Death Dis.* 2022;13:132.
- Lombard DB, Zwaans BMM. SIRT3: As simple as it seems? *Gerontology.* 2014;60:56–64.
- Schwer BR, North BJ, Frye RA, Ott M, Verdin E. The human silent information regulator (Sir)2 homologue hSIRT3 is a mitochondrial nicotinamide adenine dinucleotide-dependent deacetylase. *J Cell Biol.* 2002;158:647–57.
- Osborne B, Reznick J, Wright LE, Sinclair DA, Cooney GJ, Turner N. Liver-specific overexpression of SIRT3 enhances oxidative metabolism, but does not impact metabolic defects induced by high fat feeding in mice. *Biochem Biophys Res Commun.* 2022;607:131–7.
- Lynoe N, Sandlund M, Dahlqvist G, Jacobsson L. Informed consent: Study of quality of information given to participants in a clinical trial. *BMJ.* 1991;303:610–3.
- Khodayari N, Oshins R, Holliday LS, Clark V, Xiao Q, Marek G, et al. Alpha-1 antitrypsin deficient individuals have circulating extracellular vesicles with profibrogenic cargo. *Cell Commun Signal.* 2020;18:140.
- Khodayari N, Wang RL, Oshins R, Lu Y, Millett M, Aranyos AM, et al. The mechanism of mitochondrial injury in alpha-1 antitrypsin deficiency mediated liver disease. *Int J Mol Sci.* 2021;22:13255.

22. Khodayari N, Wang RL, Marek G, Krotova K, Kirst M, Liu C, et al. SVIP regulates Z variant alpha-1 antitrypsin retro-translocation by inhibiting ubiquitin ligase gp78. *PLoS One*. 2017;12:e0172983.
23. Hallows WC, Lee S, Denu JM. Sirtuins deacetylate and activate mammalian acetyl-CoA synthetases. *Proc Natl Acad Sci USA*. 2006;103:10230–5.
24. Borel F, Sun H, Zieger M, Cox A, Cardozo B, Li W, et al. Editing out five *Serpina1* paralogs to create a mouse model of genetic emphysema. *Proc Natl Acad Sci USA*. 2018;115:2788–93.
25. Khodayari N, Oshins R, Aranyos AM, Duarte S, Mostofizadeh S, Lu Y, et al. Characterization of hepatic inflammatory changes in a C57BL/6J mouse model of alpha1-antitrypsin deficiency. *Am J Physiol Gastrointest Liver Physiol*. 2022;323:G594–608.
26. Younossi ZM, Stepanova M, Afendy M, Fang Y, Younossi Y, Mir H, et al. Changes in the prevalence of the most common causes of chronic liver diseases in the United States from 1988 to 2008. *Clin Gastroenterol Hepatol*. 2011;9:524–530.e521; quiz e560.
27. Eskelinen EL, Illert AL, Tanaka Y, Schwarzmann G, Blanz J, Von Figura K, et al. Role of LAMP-2 in lysosome biogenesis and autophagy. *Mol Biol Cell*. 2002;13:3355–68.
28. Zhang T, Liu J, Shen S, Tong Q, Ma X, Lin L. SIRT3 promotes lipophagy and chaperon-mediated autophagy to protect hepatocytes against lipotoxicity. *Cell Death Differ*. 2020;27:329–44.
29. Motomura W, Inoue M, Ohtake T, Takahashi N, Nagamine M, Tanno S, et al. Up-regulation of ADRP in fatty liver in human and liver steatosis in mice fed with high fat diet. *Biochem Biophys Res Commun*. 2006;340:1111–8.
30. Teckman JH. Liver disease in alpha-1 antitrypsin deficiency: Current understanding and future therapy. *COPD*. 2013;10(suppl 1):35–43.
31. Fu DA, Campbell-Thompson M. Periodic acid-Schiff staining with diastase. *Methods Mol Biol*. 2017;1639:145–9.
32. Clark VC, Marek G, Liu C, Collinworth A, Shuster J, Kurtz T, et al. Clinical and histologic features of adults with alpha-1 antitrypsin deficiency in a non-cirrhotic cohort. *J Hepatol*. 2018;69:1357–64.
33. Miravittles M, Herr C, Ferrarotti I, Jardi R, Rodriguez-Frias F, Luisetti M, et al. Laboratory testing of individuals with severe alpha1-antitrypsin deficiency in three European centres. *Eur Respir J*. 2010;35:960–8.
34. Middleton P, Vergis N. Mitochondrial dysfunction and liver disease: Role, relevance, and potential for therapeutic modulation. *Therap Adv Gastroenterol*. 2021;14:17562848211031394.
35. Degechisa ST, Dabi YT, Gizaw ST. The mitochondrial associated endoplasmic reticulum membranes: A platform for the pathogenesis of inflammation-mediated metabolic diseases. *Immun Inflamm Dis*. 2022;10:e647.
36. D'Acunzo P, Pérez-González R, Kim Y, Hargash T, Miller C, Aildred MJ, et al. Mitovesicles are a novel population of extracellular vesicles of mitochondrial origin altered in Down syndrome. *Sci Adv*. 2021;7:eabe5085.
37. Pérez-Treviño P, Velásquez M, García N. Mechanisms of mitochondrial DNA escape and its relationship with different metabolic diseases. *Biochim Biophys Acta*. 2020;1866:165761.
38. Puhm F, Afonyushkin T, Resch U, Obermayer G, Rohde M, Penz T, et al. Mitochondria are a subset of extracellular vesicles released by activated monocytes and induce type I IFN and TNF responses in endothelial cells. *Circ Res*. 2019;125:43–52.
39. Marcus NY, Blomenkamp K, Ahmad M, Teckman JH. Oxidative stress contributes to liver damage in a murine model of alpha-1-antitrypsin deficiency. *Exp Biol Med (Maywood)*. 2012;237:1163–72.
40. Garrido-Pérez N, Vela-Sebastián A, López-Gallardo E, Emperador S, Iglesias E, Meade P, et al. Oxidative phosphorylation dysfunction modifies the cell secretome. *Int J Mol Sci*. 2020;21:3374.
41. Meng H, Yan WY, Lei YH, Wan Z, Hou YY, Sun LK, et al. SIRT3 regulation of mitochondrial quality control in neurodegenerative diseases. *Front Aging Neurosci*. 2019;11:313.
42. Jarc E, Petan T. Lipid droplets and the management of cellular stress. *Yale J Biol Med*. 2019;92:435–52.
43. Bosma M, Dapito DH, Drosatos-Tampakaki Z, Huiping-Son N, Huang LS, Kersten S, et al. Sequestration of fatty acids in triglycerides prevents endoplasmic reticulum stress in an in vitro model of cardiomyocyte lipotoxicity. *Biochim Biophys Acta*. 2014;1841:1648–55.
44. Cheng Y, Mai J, Hou T, Ping J. MicroRNA-421 induces hepatic mitochondrial dysfunction in non-alcoholic fatty liver disease mice by inhibiting sirtuin 3. *Biochem Biophys Res Commun*. 2016;474:57–63.
45. He J, Hu B, Shi X, Weidert ER, Lu P, Xu M, et al. Activation of the aryl hydrocarbon receptor sensitizes mice to nonalcoholic steatohepatitis by deactivating mitochondrial sirtuin deacetylase Sirt3. *Mol Cell Biol*. 2013;33:2047–55.
46. Tong W, Ju L, Qiu M, Xie Q, Chen Y, Shen W, et al. Liraglutide ameliorates non-alcoholic fatty liver disease by enhancing mitochondrial architecture and promoting autophagy through the SIRT1/SIRT3-FOXO3a pathway. *Hepatol Res*. 2016;46:933–43.
47. Li R, Xin T, Li D, Wang C, Zhu H, Zhou H. Therapeutic effect of Sirtuin 3 on ameliorating nonalcoholic fatty liver disease: The role of the ERK-CREB pathway and Bnip3-mediated mitophagy. *Redox Biol*. 2018;18:229–43.

How to cite this article: Poole B, Oshins R, Huo Z, Aranyos A, West J, Duarte S, et al. Sirtuin3 promotes the degradation of hepatic Z alpha-1 antitrypsin through lipophagy. *Hepatol Commun*. 2024;8:e0370. <https://doi.org/10.1097/HC9.0000000000000370>